THE PROPAGATION OF PLANE WAVES IN PLASTIC SOLIDS

G. J. COOPER and J. W. CRAGGS

(Received 26 October 1964)

Abstract

Equations describing a possible mode of propagation of plane waves in isotropic plastic solids are solved numerically.

Introduction

Most of the experimental work available on the propagation of waves in materials has aimed to produce longitudinal waves in wires or rods [Bell (1956), (1961a), (1961b)]. In such experiments it is possible to make detailed measurements of the longitudinal strain on the surface as a function of time. It is known that, for high rates of strain, a one dimensional analysis of the results is not satisfactory [Love (1931), p. 428] and yet a complete mathematical analysis is extremely difficult. It has therefore been almost impossible to deduce any general properties of materials at high rates of strain from experiments of this kind. The few problems for which a complete analysis is possible are either very difficult to reproduce in practice or are not susceptible of detailed measurement.

Although a complete mathematical analysis is not normally possible, tensor equations may be derived which describe the propagation of waves in some simple model of a material. Our aim is to numerically solve these equations for a particular model. For this model we assume that there is no significant difference in the behaviour of the material at different rates of strain. It has not been possible to extend the numerical results sufficiently to allow of a complete comparison with experimental data. However, so far as a comparison is possible, the results suggest that rate of strain effects are not significant.

It is assumed that a two dimensional analysis is sufficient to give agreement between numerical and experimental results. This is certainly so, close to the impact surface, and the major discrepancy appears to be due to the type of stress strain relation used.

The model

We consider an isotropic material with stress tensor σ_{ij} defined relative to a Cartesian coordinate system x_i; $i, j = 1, 2, 3$. Define a yield surface

$$f(\sigma_{ij}) = K,$$

such that for increasing f, the material behaves elastically for $f < K$ and plastically for $f \geqq K$. In general f, K may depend on the previous history of deformation of the material and may vary from point to point. We shall deal with work hardening materials for which f is a definite function of its arguments and K increases as work is done on the material. The yield surface sets a limit on the stresses for which the material behaves elastically but gives no direct information on the plastic behaviour. Stress strain relations must be the subject of further assumptions. We assume that there is a plastic potential that coincides with the yield function, f. The strain may then be divided into two tensors, the elastic strain, e_{ij}, and the plastic strain, η_{ij}, such that

$$\varepsilon_{ij} = e_{ij} + \eta_{ij} = \tfrac{1}{2}\left(\frac{\partial u_i}{\partial x_j} + \frac{\partial u_j}{\partial x_i}\right),$$

the u_i representing displacements in the x_i directions.

For elastic deformation $\dot{\eta}_{ij} = 0$, the superposed dot denoting the partial derivative with respect to time. Also, for elastic deformation,

$$e_{ij} = \frac{1+\nu}{E}\sigma_{ij} - \frac{\nu}{E}\delta_{ij}\sigma_{kk}, \tag{1}$$

where E is Young's modulus, ν Poisson's ratio, and δ_{ij} the unit tensor. In terms of reduced stress, σ'_{ij},

$$\begin{aligned} e_{ij} &= \frac{1+\nu}{E}\sigma'_{ij} + \frac{1-2\nu}{3E}\delta_{ij}\sigma_{kk}, \\ \sigma'_{ij} &= \sigma_{ij} - \tfrac{1}{3}\delta_{ij}\sigma_{kk}. \end{aligned} \tag{2}$$

If the yield function is independent of the hydrostatic stress, $-\frac{1}{3}\sigma_{kk}$, plastic strain takes place without change of volume.

The plastic strain is defined by

$$\dot{\eta}_{ij} = \dot{\Lambda}\frac{\partial f}{\partial \sigma_{ij}},$$

where $\dot{\Lambda}$ is a proportionality factor which is a function of time and position. Since this equation is homogeneous and linear in the time derivative, stress and strain in the model may depend on the loading history but not on the rate of loading.

It is assumed that unloading proceeds elastically. Then, whenever

$$f < K \quad \text{or} \quad f = K, \quad \dot{f} < 0,$$

plastic strain remains constant and

$$\dot{\eta}_{ij} = 0, \quad \dot{\varepsilon}_{ij} = \dot{e}_{ij}.$$

In order to include the effect of hardening put

$$K = K(\omega), \quad \dot{\omega} = \sigma_{ij}\dot{\eta}_{ij},$$

so that $\dot{\omega}$ is the rate at which plastic work is done by external forces. Hence

$$\dot{K} = \frac{\partial f}{\partial \sigma_{ij}} \dot{\sigma}_{ij} = \frac{\partial K}{\partial \omega} \dot{\omega} = \dot{\Lambda} \frac{\partial K}{\partial \omega} \sigma_{ij} \frac{\partial f}{\partial \sigma_{ij}},$$

and $\dot{\Lambda}$ becomes determinate.

The particular model to be considered is a Prandtl-Reuss elastic-plastic material. This model has a von Mises yield surface

$$\sigma'_{ij}\sigma'_{ij} = 2k^2 = K,$$

independent of hydrostatic stress. The definition of plastic strain becomes

$$\dot{\eta}_{ij} = \dot{\Lambda}\sigma'_{ij},$$

and hence

$$\frac{\dot{\eta}_{11}}{\sigma'_{11}} = \frac{\dot{\eta}_{22}}{\sigma'_{22}} = \frac{\dot{\eta}_{33}}{\sigma'_{33}} = \frac{\dot{\eta}_{12}}{\sigma'_{12}} = \frac{\dot{\eta}_{13}}{\sigma'_{13}} = \frac{\dot{\eta}_{23}}{\sigma'_{23}},$$

thus determining the $\dot{\eta}_{ij}$ apart from a multiplicative constant. To complete the determination of $\dot{\eta}_{ij}$ and to include work hardening we have

$$\dot{\omega} = \sigma'_{ij}\dot{\eta}_{ij},$$

and hence

$$\frac{\dot{\eta}_{ij}}{\sigma'_{ij}} = \frac{\dot{\omega}}{2k^2} = \frac{\dot{k}}{2k^2 \dfrac{\partial k}{\partial \omega}} = \frac{2k\dot{k}}{4k^3 \dfrac{\partial k}{\partial \omega}} = \frac{\sigma'_{ij}\dot{\sigma}'_{ij}}{4k^3 \dfrac{\partial k}{\partial \omega}}.$$

This implies $\dot{\eta}_{kk} = 0$ so that plastic deformation takes place without change of volume. For plastic deformation

$$\dot{\varepsilon}_{ij} = \frac{1+\nu}{E} \dot{\sigma}'_{ij} + \frac{1-2\nu}{3E} \delta_{ij}\dot{\sigma}_{kk} + \sigma'_{ij} G(\sigma_{ij}), \tag{3}$$

where

$$G(\sigma_{ij}) = \frac{\sigma'_{pq}\dot{\sigma}'_{pq}}{4k^3 \dfrac{\partial k}{\partial \omega}}.$$

The material behaves elastically, $\dot{\varepsilon}_{ij} = \dot{e}_{ij}$, for

$$\sigma'_{ij}\sigma'_{ij} < 2k^2 \quad \text{or} \quad \sigma'_{ij}\sigma'_{ij} = 2k^2, \quad \sigma'_{ij}\dot{\sigma}'_{ij} < 0. \tag{4}$$

We take $2k^2$ to be the maximum value the yield function has attained in the loading history of the material at the point being considered. In the elastic-plastic transition region equations 3, 4 are consistent since $\dot{\eta}_{ij} = 0$ when $\sigma'_{pq}\dot{\sigma}'_{pq} = 0$.

Elastic deformation may be regarded as a special case, $G(\sigma_{ij}) = 0$, of plastic deformation. If the criteria given by equations 4 are not invoked, so that unloading proceeds according to equation 3, then the deformation is termed non-linear elastic.

A complete discussion is given by Hill [(1950)].

Tensor equations for plane strain

Consider a plate of Prandtl-Reuss material bounded by $x_1 = 0$, $x_2 = \pm a$ and unbounded in x_3 and the positive x_1 direction. Everywhere $\varepsilon_{13} = \varepsilon_{23} = \varepsilon_{33} = \sigma_{13} = \sigma_{23} = 0$. For a plastic or elastic region equation 3 gives

$$\dot{\varepsilon}_{11} = \frac{1+\nu}{E}\dot{\sigma}'_{11} + \frac{1-2\nu}{3E}\dot{\sigma}_{kk} + \sigma'_{11}G(\sigma_{ij}), \tag{5}$$

$$\dot{\varepsilon}_{22} = \frac{1+\nu}{E}\dot{\sigma}'_{22} + \frac{1-2\nu}{3E}\dot{\sigma}_{kk} + \sigma'_{22}G(\sigma_{ij}), \tag{6}$$

$$\dot{\varepsilon}_{12} = \frac{1+\nu}{E}\dot{\sigma}'_{12} + \sigma'_{12}G(\sigma_{ij}), \tag{7}$$

$$0 = \frac{1+\nu}{E}\dot{\sigma}'_{33} + \frac{1-2\nu}{3E}\dot{\sigma}_{kk} + \sigma'_{33}G(\sigma_{ij}). \tag{8}$$

Since $\sigma'_{kk} = 0$ the addition of equations 5, 6 and 8 gives for both elastic and plastic regions

$$\dot{\varepsilon}_{kk} = \frac{1-2\nu}{E}\dot{\sigma}_{kk}. \tag{9}$$

At this stage it is convenient to scale the stress unit to remove the factor $(1+\nu)/E$. Assume for the present that the term $2k(\partial k/\partial\omega)$, occurring in $G(\sigma_{ij})$, is similarly scaled. Then the subtraction of equation 8 from equations 5 and 6 leaves

$$\dot{\varepsilon}_{11} = 2\dot{\sigma}'_{11} + \dot{\sigma}'_{22} + (2\sigma'_{11} + \sigma'_{22})G(\sigma_{ij}), \tag{10}$$

$$\dot{\varepsilon}_{22} = \dot{\sigma}'_{11} + 2\dot{\sigma}'_{22} + (\sigma'_{11} + 2\sigma'_{22})G(\sigma_{ij}), \tag{11}$$

$$\dot{\varepsilon}_{12} = \dot{\sigma}'_{12} + \sigma'_{12}G(\sigma_{ij}). \tag{12}$$

Since $\sigma'_{ij} = \sigma_{ij} - \frac{1}{3}\delta_{ij}\sigma_{kk}$ equation 9 gives

$$\dot{\sigma}_{11} = \dot{\sigma}'_{11} + \frac{1+\nu}{3(1-2\nu)}\,[\dot{\varepsilon}_{11}+\dot{\varepsilon}_{22}], \tag{13}$$

$$\dot{\sigma}_{22} = \dot{\sigma}'_{22} + \frac{1+\nu}{3(1-2\nu)}\,[\dot{\varepsilon}_{11}+\dot{\varepsilon}_{22}]. \tag{14}$$

Also

$$\dot{\sigma}_{12} = \dot{\sigma}'_{12}, \tag{15}$$

$$\dot{\sigma}_{33} = -\tfrac{3}{2}(\dot{\sigma}'_{11}+\dot{\sigma}'_{22})+\tfrac{1}{2}(\dot{\sigma}_{11}+\dot{\sigma}_{22}). \tag{16}$$

For an elastic region these equations reduce to

$$\dot{\sigma}_{11} = \frac{1}{1-2\nu}\,[(1-\nu)\dot{\varepsilon}_{11}+\nu\dot{\varepsilon}_{22}], \tag{17}$$

$$\dot{\sigma}_{22} = \frac{1}{1-2\nu}\,[\nu\dot{\varepsilon}_{11}+(1-\nu)\dot{\varepsilon}_{22}], \tag{18}$$

$$\dot{\sigma}_{12} = \dot{\varepsilon}_{12}, \tag{19}$$

$$\dot{\sigma}_{33} = \nu(\dot{\sigma}_{11}+\dot{\sigma}_{22}). \tag{20}$$

Equations are still required to determine whether the region is elastic or plastic. These equations are used to decide if $G(\sigma_{ij})$ should be set to zero, that is, whether equations 10—16 or 17—20 are to be used to evaluate the stress derivatives. We have

$$f = \sigma'_{pq}\sigma'_{pq} = 2\sigma'^2_{11}+2\sigma'^2_{22}+2\sigma'^2_{12}+2\sigma'_{11}\sigma'_{22}, \tag{21}$$

and

$$\sigma'_{pq}\dot{\sigma}'_{pq} = \sigma'_{11}(2\dot{\sigma}'_{11}+\dot{\sigma}'_{22})+\sigma'_{22}(2\dot{\sigma}'_{22}+\dot{\sigma}'_{11})+2\sigma'_{12}\dot{\sigma}'_{12}.$$

This second equation requires the values of $\dot{\sigma}'_{ij}$ and these are not known at the state that this equation is used. In practice this difficulty has been avoided by assuming the region to be plastic whence

$$\sigma'_{pq}\dot{\sigma}'_{pq} = (\sigma'_{11}\dot{\varepsilon}_{11}+\sigma'_{22}\dot{\varepsilon}_{22}+2\sigma'_{12}\dot{\varepsilon}_{12})\left[1+\frac{\sigma'^2_{11}+\sigma'^2_{22}+\sigma'_{11}\sigma'_{22}+\sigma'^2_{12}}{2k^3\dfrac{\partial k}{\partial \omega}}\right]^{-1} \tag{22}$$

If the region turns out to be elastic then, after applying equations 17—20, $\sigma'_{pq}\dot{\sigma}'_{pq}$ is checked.

Dynamical and compatibility equations

The tensor equations already derived must be solved in conjunction with the dynamical equations [Sokolnikoff, (1946), p. 82]. Let ρ denote the

https://doi.org/10.1017/S1446788700027774 Published online by Cambridge University Press

density. Then, since the body forces are zero

$$\rho \ddot{u}_i = \frac{\partial \sigma_{ij}}{\partial x_j}; \qquad i, j = 1, 2.$$

Scale the time coordinate to remove the factor ρ, differentiate with respect to x_i, x_j and sum. Then

$$(23) \qquad 2\ddot{\varepsilon}_{ij} = \frac{\partial^2 \sigma_{ik}}{\partial x_j \partial x_k} + \frac{\partial^2 \sigma_{jk}}{\partial x_i \partial x_k} \qquad ; i, j, k = 1, 2.$$

The Saint-Venant compatibility equations [Love (1931), p. 49] are valid for both elastic and plastic regions. For plane strain these equations reduce to

$$(24) \qquad 0 = \frac{\partial^2 \varepsilon_{11}}{\partial x_2^2} - 2\frac{\partial^2 \varepsilon_{12}}{\partial x_1 \partial x_2} + \frac{\partial^2 \varepsilon_{22}}{\partial x_1^2}.$$

This equation may be used to check the numerical results.

The stress strain relation

The simplest types of experiment for determining stress strain relations are experiments involving pure shear only, such as torsion experiments where

$$\varepsilon_{12} = F(\sigma_{12}),$$

all σ_{ij}, except $\sigma_{12} = \sigma_{21}$, being zero.

Data and graphs are available from such experiments [Wilkins and Bunn [(1943), p. 7] and, suggest that a suitable functional relationship between σ_{12} and ε_{12} is given by

$$(25) \qquad \sigma_{12} = \frac{\varepsilon_{12}}{\sqrt{1+2\theta\varepsilon_{12}^2}} \text{ in scaled stress units.}$$

This relation gives the approximate shape of the stress strain curve for various copper alloys with some possible variation in the slope of the asymptote. Bell [(1959)] gives a static stress strain curve for annealed aluminium which differs substantially from this type of relation both as regards the slope of the asymptote and the degree of curvature. The parabolic relation given by equation 25 is used since it appears to be the easiest to handle. Second order terms, although omitted in the numerator must be included under the square root sign.

From equation 25

$$\varepsilon_{12} = \frac{\sigma_{12}}{\sqrt{1-2\theta\sigma_{12}^2}}$$

and therefore

$$\frac{1}{2k\dfrac{\partial k}{\partial \omega}} = (1-2\theta k^2)^{-\frac{3}{2}}-1. \tag{26}$$

This equation is assumed to hold for general stresses and strains.

Initial and boundary values

Assume that a shock of constant force is applied at time $t = 0$, the force being applied in the direction of increasing x_1. Then for

$$t \leqq 0, \quad x_1 > 0, \quad \text{all} \quad x_2,$$

all stresses and strains are zero;

$$\begin{aligned} &t \geqq 0, x_1 = 0, \quad \text{all } x_2, \\ &\sigma_{12} = \sigma_{22} = 0, \quad \sigma_{11} = \sigma, \quad \text{where } \sigma \text{ is a constant;} \\ &t \geqq 0, \text{ all } x_1, x_2 = \pm a, \\ &\sigma_{12} = \sigma_{22} = 0. \end{aligned}$$

The end conditions for large t are given by

$$\sigma_{11} = \sigma, \quad \sigma_{12} = \sigma_{22} = 0, \quad \text{for all } x_1, x_2.$$

The propagated waves are symmetric about $x_1 = 0$ so that the equations need only be solved for positive x_2.

It has not been possible to include the boundary conditions in the dynamical equations in such a fashion that the resulting differential equations can be solved on the boundary by stable numerical process. Therefore on the boundary the method of solution that has been used is similar to that used for the interior of the plate. The stresses σ_{12}, σ_{22} are set to zero.

It does not appear to be as simple to use a boundary condition on the impact face corresponding to a constant velocity impact.

Numerical solution of the equations

The partial differential equations, 23, are a set of simultaneous equations of hyperbolic type. These equations may be replaced by finite difference approximations. The resulting difference equations may then be solved, for a rectangular mesh corresponding to the plate, by a stepping ahead procedure in time. The mesh points are labelled by three indices l, m, n,

$$t = l\delta t, \qquad l = 0, 1, 2, \cdots,$$
$$x_1 = m\delta x_1, \quad m = 0, 1, 2, \cdots,$$
$$x_2 = n\delta x_2, \quad n = 0, 1, \cdots \frac{a}{\delta x_2} = N,$$

where δt, δx_1, δx_2, are constant increments in t, x_1, x_2. We choose $\delta x = \delta x_1 = \delta x_2$ and δt must be chosen sufficiently small to guard against the possible accumulation of rounding errors. The indices are placed in square brackets after the variable. Where there is no likelihood of misinterpretation some or all the indices may be omitted.

The method used to solve the equations is essentially as follows. Assume that, for time intervals l and $l-1$,

$$\sigma_{11}, \sigma_{22}, \sigma_{12}, \sigma_{33}, \varepsilon_{11}, \varepsilon_{22}, \varepsilon_{12}, 2k^2,$$

are known for all $m > 0$ and for all n. For $m = 0$, only

$$\sigma_{11}, \sigma_{22}, \sigma_{12},$$

are required. Then for each pair of permissible values of m and n, $m > 0$, we proceed in the following fashion.

The difference equations derived from the dynamical equations, 23, give $\varepsilon_{ij}[l+1]$ and $2\delta t\dot{\varepsilon}_{ij}[l]$. From equations 2, $\sigma'_{ij}[l]$ are determined and then $4k^3(\partial k/\partial\omega)$ $[l]$ may be evaluated using equation 26. Hence $2\delta t\sigma'_{pq}\dot{\sigma}'_{pq}$ $[l]$ may be determined from equation 22. This procedure is used both for interior and boundary points. If $2k^2[l] > 2k^2[l-1]$ or $2\delta t\sigma'_{pq}\dot{\sigma}'_{pq}[l] \geqq 0$ the plastic equations, 10 to 16, are now used to compute values for $2\delta t\dot{\sigma}_{ij}[l]$. Otherwise the elastic equations, 17 to 20, are used. At this stage, for points on the boundary $x_2 = a$, the conditions $\dot{\sigma}_{22} = \dot{\sigma}_{12} = 0$ are enforced and the value of $\dot{\sigma}_{33}$, computed from equation 16 or 20, altered suitably. When the elastic equations are used $2\delta t\sigma'_{pq}\dot{\sigma}'_{pq}[l]$ is now recomputed and if $2\delta t\sigma'_{pq}\dot{\sigma}'_{pq}[l] \geqq 0$ then this value and the values of l, m, n are retained for investigation. From the values of $\sigma_{ij}[l]$ and $2\delta t\dot{\sigma}_{ij}[l]$, the stresses $\sigma_{ij}[l+1]$ are determined. Hence $\sigma'_{pq}\sigma'_{pq}[l+1]$ is evaluated using equations 2 and 21. The maximum value of $2k^2[l]$ and $\sigma'_{pq}\sigma'_{pq}[l+1]$ determines $2k^2[l+1]$. Values for

$$\sigma_{11}, \sigma_{22}, \sigma_{12}, \sigma_{33}, \varepsilon_{11}, \varepsilon_{22}, \varepsilon_{12}, 2k^2,$$

have no been determined for the time interval $l+1$ for each pair of values m, n, so that the procedure may be repeated for the next interval in time.

Finite difference approximations

The difference approximations used may be obtained from most standard texts on numerical analysis either explicitly [Buckingham (1957)] or

https://doi.org/10.1017/S1446788700027774 Published online by Cambridge University Press

derived by use of Taylor series or finite difference operators [Milne (1949)]. We give the approximations used for the required partial derivatives of a function $f(t, x_1, x_2)$ known at points of the mesh.

We have

$$\frac{\partial f}{\partial t}[l] = \frac{f[l+1]-f[l-1]}{2\delta t} + 0(\delta t^2),\ l > 0,$$

$$\frac{\partial^2 f}{\partial t^2}[l] = \frac{f[l+1]-2f[l]+f[l-1]}{\delta t^2} + 0(\delta t^2),\ l > 0.$$

The functions which concern us are zero for $l \leqq 0$ and hence the second approximation is valid for all l. For $l = 0$ the factor $\frac{1}{2}$ should strictly be omitted from the first approximation. But, since this approximation is used to compute $2\delta t \dot{\varepsilon}_{ij}[l]$ from $\varepsilon_{ij}[l+1]$ and $\varepsilon_{ij}[l-1]$ and then used to compute $\sigma_{ij}[l+1]$ from $2\delta t \dot{\sigma}_{ij}[l]$ and $\sigma_{ij}[l-1]$, the factor may be retained. Hence, apart from ensuring that the functions are everywhere zero for $l = 0$, $l = -1$, no special starting procedure is required. Similar approximations are used for

$$\frac{\partial^2 f}{\partial x_1^2}[m] \text{ for } m > 0,$$

$$\frac{\partial^2 f}{\partial x_2^2}[n] \text{ for } 0 < n < N.$$

For $n = 0$ the approximation holds if $f[1]$ is substituted for $f[-1]$ since there is symmetry across $n = 0$. For $n = N$ the following approximation, using backward differences, is needed.

$$\frac{\partial^2 f}{\partial x_2^2}[N] = \frac{2f[N]-5f[N-1]+4f[N-2]-f[N-3]}{\delta x^2} + 0(\delta x^2).$$

$$\frac{\partial^2 f}{\partial x_1 \partial x_2}[m, n] = \frac{f[m+1, n+1]-f[m+1, n-1]-f[m-1, n+1]+f[m-1, n-1]}{4\delta x^2} + 0(\delta x^2),\ 0 < n < N.$$

For $n = 0$ this approximation holds with $f[m \pm 1, 1]$ substituted for $f[m \pm 1, -1]$. For $n = N$ we use

$$\frac{\partial^2 f}{\partial x_1 \partial x_2}[m, N] = \frac{3f[m+1, N]-3f[m-1, N]+f[m+1, N-2]-f[m-1, N-2]}{4\delta x^2} + \frac{f[m-1, N-1]-f[m+1, N-1]}{\delta x^2} + 0(\delta x^2).$$

Results given later were all obtained using these difference approximations and difference checks showed that fourth order differences were small. Results have also been obtained using simpler difference approximations on the boundary with truncation errors of the order of δx. No significant difference has been observed provided $N \geqq 7$.

Difference equations

Using these finite difference approximations the following difference equations are obtained from the dynamical equations 23.

For $l \geqq 0, m > 0, 0 < n < N$,

$$\begin{aligned}\varepsilon_{11}[l+1, m, n] = {} & 2\varepsilon_{11}[l, m, n]-\varepsilon_{11}[l-1, m, n] \\ & +\left(\frac{\delta t}{\delta x}\right)^2(\sigma_{11}[l, m+1, n]-2\sigma_{11}[l, m, n]+\sigma_{11}[l, m-1, n]) \\ & +\tfrac{1}{4}\left(\frac{\delta t}{\delta x}\right)^2(\sigma_{12}[l, m+1, n+1]-\sigma_{12}[l, m+1, n-1] \\ & \quad -\sigma_{12}[l, m-1, n+1]+\sigma_{12}[l, m-1, n-1]) \\ & \quad +0(\delta t^2\delta x^2);\end{aligned}$$

$$\begin{aligned}\varepsilon_{22}[l+1, m, n] = {} & 2\varepsilon_{22}[l, m, n]-\varepsilon_{22}[l-1, m, n] \\ & +\left(\frac{\delta t}{\delta x}\right)^2(\sigma_{22}[l, m, n+1]-2\sigma_{22}[l, m, n]+\sigma_{22}[l, m, n-1]) \\ & +\tfrac{1}{4}\left(\frac{\delta t}{\delta x}\right)^2(\sigma_{12}[l, m+1, n+1]-\sigma_{12}[l, m+1, n-1] \\ & \quad -\sigma_{12}[l, m-1, n+1]+\sigma_{12}[l, m-1, n-1])+0(\delta t^2\delta x^2);\end{aligned}$$

$$\begin{aligned}\varepsilon_{12}[l+1, m, n] = {} & 2\varepsilon_{12}[l, m, n]-\varepsilon_{12}[l-1, m, n] \\ & +\tfrac{1}{2}\left(\frac{\delta t}{\delta x}\right)^2(\sigma_{12}[l, m+1, n]+\sigma_{12}[l, m-1, n]+\sigma_{12}[l, m, n+1] \\ & \quad +\sigma_{12}[l, m, n-1]-4\sigma_{12}[l, m, n]) \\ & +\tfrac{1}{8}\left(\frac{\delta t}{\delta x}\right)^2((\sigma_{11}+\sigma_{22})[l, m+1, n+1] \\ & \quad -[\sigma_{11}+\sigma_{22})[l, m+1, n-1]-(\sigma_{11}+\sigma_{22})[l, m-1, n+1] \\ & \quad +(\sigma_{11}+\sigma_{22})[l, m-1, n-1])+0(\delta t^2\delta x^2).\end{aligned}$$

On the axis $x_1 = 0$ these difference equations are valid if $n+1$ is substituted for $n-1$. For $l \geqq 0, m > 0, n = N$,

https://doi.org/10.1017/S1446788700027774 Published online by Cambridge University Press

$$\begin{aligned}
\varepsilon_{11}[l+1, m, N] = {} & 2\varepsilon_{11}[l, m, N]-\varepsilon_{11}[l-1, m, N] \\
& +\left(\frac{\delta t}{\delta x}\right)^2 (\sigma_{11}[l, m+1, N]-2\sigma_{11}[l, m, N]+\sigma_{11}[l, m-1, N]) \\
& +\tfrac{1}{4}\left(\frac{\delta t}{\delta x}\right)^2 (-4\sigma_{12}[l, m+1, N-1]+4\sigma_{12}[l, m-1, N-1] \\
& \quad +\sigma_{12}[l, m+1, N-2]-\sigma_{12}[l, m-1, N-2])+0(\delta t^2 \delta x^2);
\end{aligned}$$

$$\begin{aligned}
\varepsilon_{22}[l+1, m, N] = {} & 2\varepsilon_{22}[l, m, N]-\varepsilon_{22}[l-1, m, N] \\
& +\left(\frac{\delta t}{\delta x}\right)^2 (-5\sigma_{22}[l, m, N-1]+4\sigma_{22}[l, m, N-2] \\
& \quad -\sigma_{22}[l, m, N-3]) \\
& +\tfrac{1}{4}\left(\frac{\delta t}{\delta x}\right)^2 (-4\sigma_{12}[l, m+1, N-1]+4\sigma_{12}[l, m-1, N-1] \\
& \quad +\sigma_{12}[l, m+1, N-2]-\sigma_{12}[l, m-1, N-2])+0(\delta t^2 \delta x^2);
\end{aligned}$$

$$\begin{aligned}
\varepsilon_{12}[l+1, m, N] = {} & 2\varepsilon_{12}[l, m, N]-\varepsilon_{12}[l-1, m, N] \\
& +\left(\frac{\delta t}{\delta x}\right)^2 (-5\sigma_{12}[l, m, N-1]+4\sigma_{12}[l, m, N-2] \\
& \quad -\sigma_{12}[l, m, N-3]) \\
& +\tfrac{1}{4}\left(\frac{\delta t}{\delta x}\right)^2 (3\sigma_{11}[l, m+1, N]-3\sigma_{11}[l, m-1, N] \\
& \quad -4(\sigma_{11}+\sigma_{22})[l, m+1, N-1] \\
& \quad +4(\sigma_{11}+\sigma_{22})[l, m-1, N-1]+(\sigma_{11}+\sigma_{22})[l, m+1, N-2] \\
& \quad -(\sigma_{11}+\sigma_{22})[l, m-1, N-2])+0(\delta t^2 \delta x^2).
\end{aligned}$$

It follows from equation 12 that $\varepsilon_{12} = 0$ on the boundary and therefore this last difference equation serves as a check on the numerical process. It does not appear to be feasible to apply a Mesh Fourier analysis to these difference equations, and hence to obtain bounds on the ratio $\delta t/\delta x$ which ensure numerical stability. Estimates may be obtained by comparison with the problem of pure elastic deformation, which is the special case $\theta = 0$. It can then be shown that the dynamical equations may be expressed as a pair of wave equations with a fast wave velocity.

$$c_1 = \sqrt{\frac{1-\nu}{1-2\nu}},$$

and a slow wave velocity

https://doi.org/10.1017/S1446788700027774 Published online by Cambridge University Press

$$c_2 = \frac{1}{\sqrt{2}}.$$

This indicates a likelihood of numerical stability when

$$\frac{\delta t}{\delta x} < \frac{1}{c_1}.$$

Difference approximations to the elastic equations have been subjected to a Mesh Fourier analysis and this has confirmed this estimate. Numerical results also confirm the estimate. Numerical results for plastic deformation indicate that the fast wave velocity is virtually identical with that for pure elastic deformation and also that oscillations are introduced if the bound is exceeded. For Poisson's ratio $\frac{1}{3}$ the bound is

$$\left(\frac{\delta t}{\delta x}\right)^2 < \tfrac{1}{2}.$$

Results given later have all been obtained using

$$\eta = \left(\frac{\delta t}{\delta x}\right)^2 = \tfrac{1}{4}.$$

Programs

The computations have been performed on the Ferranti Pegasus digital computer installed at Leeds University. To obtain reasonable operating speed and efficient use of storage space it was necessary to program the machine in basic code. As a comprehensive check another program was written in an autocode language and results compared for the first 20 intervals in time. Results for the first few time intervals were also obtained by hand computation. Comparison of results was exact to within machine rounding errors. This alone would indicate that errors are not propagated through the system in an accumulative fashion.

The programs were written so that results could be obtained for the propagation of waves in plastic materials and also in elastic materials with both linear and nonlinear stress strain curves. The results for linear elasticity agree with those obtained from an earlier basic code program. This program was based on a slightly different mathematical analysis, the equations being expressed in terms of displacements. A boundary condition corresponding to a constant velocity impact was imposed and this presumably accounts for the minor differences observed.

Due to the comparative slowness of the autocode programs, most checks were carried out for $N = 3$. Results detailed later were obtained for $N = 7$, corresponding to a total of 14 intervals across the plate. Results for $N \geqq 7$ differed only slightly.

The machine used has a small high speed store and a large backing store. Program and data in the backing store must be transferred to the high speed store before use and transfers can be carried out in blocks of eight 39 bit words. Since eight variables are required for each mesh point one block was associated with each point. All variables for all mesh points for the last two time planes, l, $l-1$, evaluated are stored in the backing store. When the new variables for the time plane $l+1$ are calculated they are stored in place of the $l-1$ plane. The principal limitation on the basic code program is one of storage. With $N = 7$ roughly the first 100 time intervals may be computed.

The program is divided into three parts. The first section clears the whole of the store, reads in the parameters required (in particular, ν, θ, η, N, and some print parameters) and stores them. The second part deals with the evaluation of all the difference equations and tensor equations for the stresses. As much of this section as possible (roughly one half) has been fitted into the high speed store. For one time plane this section evaluates the eight variables for all the intervals in x_2 for successive intervals in x_1 until all the strains for an interval in x_1 are zero or until storage space has been exhausted. The third part, the print section, is then called in to decide what information, if any, is to be printed and to output it in a suitable format. Control is then returned to the second section which proceeds with calculations for the next time interval. If required all relevant information may first be stored on magnetic tape so that the calculations may be restarted from some time interval other than $l = 0$.

The tensor equations for an elastic region have been treated separately to those for a plastic region. This is not necessary but provides a useful check. Results obtained for elastic deformation using the elastic equations agree with those obtained using the plastic equations with $\theta = 0$.

Other facilities that have been included are concerned with checking procedures. The St. Venant compatibility equation 24 has been replaced by a finite difference approximation and values obtained for the left hand side may be printed for selected mesh points. It has been pointed out that the strain ε_{12} should be zero on the boundary and the print section prints all three strains ε_{11}, ε_{22}, ε_{12} on the boundary. On the boundary the stress σ_{22}, σ_{12} are forced to zero having previously been computed by the same procedure used for interior mesh points. The values obtained by this procedure may be printed and, as the numerical solution is expected to behave smoothly, should be small.

There is some danger of overflow when working in fixed point arithmetic. It was expected that the maximum stresses likely to occur would be some 10% higher than the initial applied stress, σ. This was therefore kept small. No estimate of the maximum strains could be obtained. However as far as the numerical calculations have been taken a value of σ of 0.125 has been satisfactory. There is some indication that if the calculations were taken further the strains would increase to a point where overflow would occur. There are two problems to be considered when computing $G(\sigma_{ij})$. Equation 26 shows that if the stresses become large $2\theta k^2$ approaches unity. This causes a loss of significant figures and cannot be prevented. Also since the computations involve rounding errors $2\theta k^2$ may actually be evaluated as slightly greater than unity thus causing overflow. This only happens when working high up on the stress strain curve and it can be assumed that $2k^2$ is constant and hence $\sigma'_{pq}\dot{\sigma}'_{pq} = 0$. That is, $G(\sigma_{ij}) = 0$. As $2\theta k^2$ approaches unity $2k(\partial k/\partial \omega)$ becomes large so that care must be exercised in computing $G(\sigma_{ij})$ in order to avoid overflow.

It can be shown using equation 21 that for $\sigma = \cdot 125$ the maximum permissible value of θ is 128. For $\theta \leqq 60$ the problems mentioned in the previous paragraph have not been important.

Results

The results given here have all been obtained using $\nu = \frac{1}{3}$, $N = 7$, $\eta = \frac{1}{4}$, $\sigma = \frac{1}{8}$. All the checks mentioned have been carried out and have proved satisfactory. In particular St. Venant's compatibility equation is approximately satisfied and the boundary stresses σ_{22}, σ_{12} approximate to zero. The errors involved are, except near the impact face, an order of magnitude less than the maximum strains or stresses at the mesh point considered. In all the graphs the strain, ε_{11}, has been plotted against time at a half and one, plate width from the impact face. The velocity of sound in aluminium is approximately 5000 metres/sec and for a plate of width one inch it can be shown that for $N = 7$, $\eta = \frac{1}{4}$, $\delta t \simeq 0.2\ \mu$s.

Graph 1 gives results obtained for pure elastic deformation. These results compare reasonably with previous results obtained for $\nu = \frac{1}{4}$ and a constant velocity impact although the oscillations are less pronounced. The ratio of the times taken for the strain to build up to the first peak and to the second peak is very close to the ratio of the two wave velocities c_1, c_2. The strain level should settle down to an asymptotic limit given by the end conditions imposed on equations 17, 18. This gives

$$\lim_{t\to\infty} \varepsilon_{11} = (1-\nu)\sigma,$$
$$= \tfrac{1}{12}.$$

Graph 2 gives results for plastic deformation with $\theta = 120$. These results may be compared with experimental data [Bell [1959)]. Our model differs

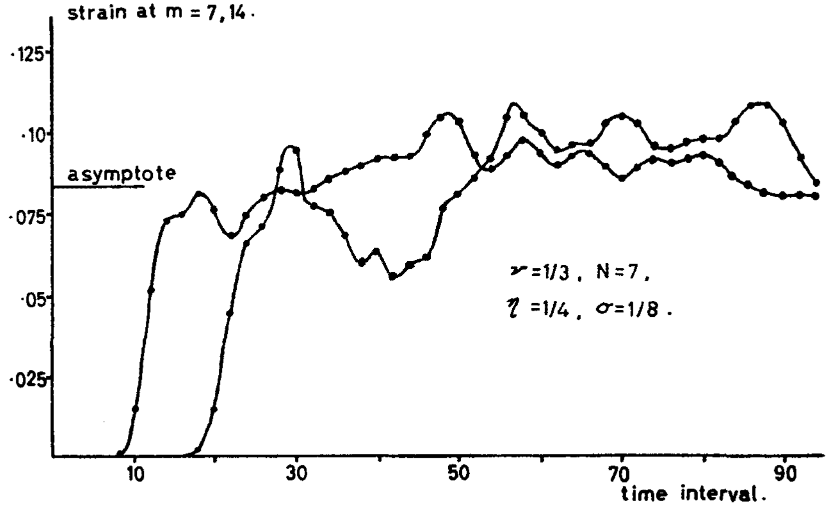

Graph 1. Elastic deformation, $\lambda = 0$.

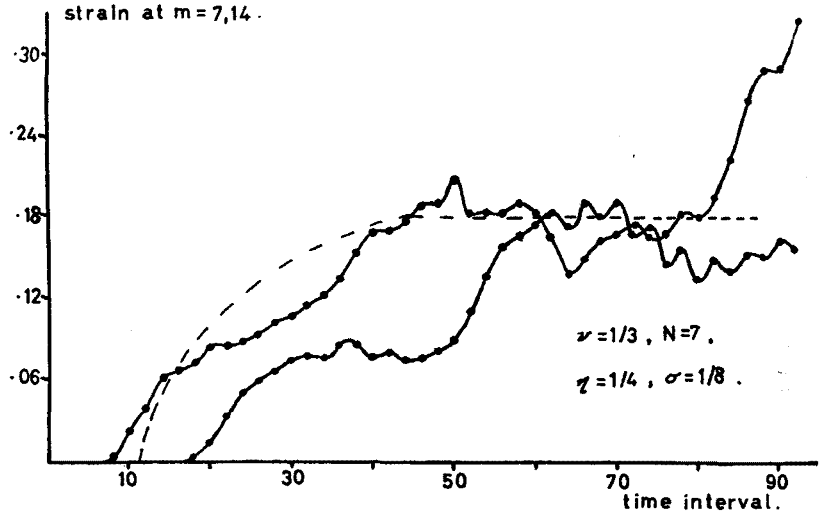

Graph 2. Plastic deformation, $\lambda = 120$.
The dotted line shows the result deduced from uniaxial stress.

from Bell's experimental approach in various ways. In particular the experiments were carried out using rods of aluminium. We have considered a two dimensional plate and a comparison of results cannot be expected to give good agreement except close to the impact face. The static stress

https://doi.org/10.1017/S1446788700027774 Published online by Cambridge University Press

strain curve obtained by Bell for a rod of aluminium has an asymptote which is not horizontal and also has a very sharp curvature away from the initial linear elastic section. A constant velocity impact is used as distinct from the constant force impact in these investigations. Nevertheless the rapid increase in strain, observed at half a plate width from the impact face at about 15μs after impact, agrees approximately with the experimentally observed increase some 10 μs after impact. It has not been possible to extend results further to determine whether or not the strain levels off as shown experimentally.

The importance or otherwise of strain rate effects cannot be decided on the basis of these results. However it does appear that at least the initial behaviour is not significantly dependent on rate of strain.

References

Bell, J. F., 1956, 1959, Journ. App. Physics, 27, 10, 30, 2.
Bell, J. F., 1961 a, b, J. Mech. Phys. Solids, 9, pp. 1—15, 261—278.
Buckingham, R. A., 1957, Numerical Methods, Pitman, London.
Hill, R., 1950, The Mathematical Theory of Plasticity, Clarendon Press, Oxford.
Love, A. E. H., 1934, The Mathematical Theory of Elasticity, 4th ed. Cambridge University Press, Cambridge.
Milne, E. W., 1949 Numerical Calculus, Princeton University Press, Princeton.
Sokolnikoff, I. S., 1946 Mathematical Theory of Elasticity, McGraw-Hill, New York.
Wilkins, R. A. and E. S. Bunn, 1943, Copper and Copper Base Alloys, 1st ed., McGraw-Hill, New York.

Department of Mathematics
University of Melbourne